Construction and Building Materials 157 (2017) 313–321

Contents lists available at ScienceDirect

Construction and Building Materials

journal homepage: www.elsevier.com/locate/conbuildmat

# Fatigue performance of prestressed concrete beams using BFRP bars

Taha Younes [a,*], Adil Al-Mayah [a,b], Tim Topper [a]

[a] Dept. of Civil and Env. Engineering, University of Waterloo, 200 University Ave W, Waterloo, ON N2L 3G1, Canada
[b] Dept. of Mechanical and Mechatronics Engineering, University of Waterloo, 200 University Ave W, Waterloo, ON N2L 3G1, Canada

## HIGHLIGHTS

- Basalt bars were used in prestressing concrete beams subjected to fatigue loading.
- There was little effect of prestressing on fatigue strength for low fatigue lives.
- Enough prestress was retained to close cracks for fatigue lives above 100,000 cycles.
- Prestressed beams failed by bar rupture after concrete crushing in monotonic tests.

## ARTICLE INFO

*Article history:*
Received 7 September 2016
Received in revised form 14 June 2017
Accepted 15 September 2017

*Keywords:*
BFRP bars
Prestressed concrete
Fatigue
Flexural behaviour

## ABSTRACT

Basalt fibers have recently been introduced as a promising addition to the existing fiber reinforced polymer (FRP) family. A limited amount of information is available on basalt FRP (BFRP) bars and their structural concrete applications. This paper presents the flexural behaviour of sixteen prestressed concrete beams using BFRP bars under monotonic and fatigue loading. The investigated parameters were the level of prestress of the bars (0%, 20% and 40% of their static tension capacity) and the fatigue load ranges. The experimental findings showed that beams with the bars prestressed to 40% of the bar strength had a higher fatigue strength than those prestressed to 0% and 20%. For 40% and 20% prestressed beams, there is no improvement in fatigue performance for load ranges above 20% and 13% of the ultimate capacity of the beams a level at which calculations showed that the remaining prestress did not close cracks at the minimum load in the fatigue load cycle. When compared on the basis of load range versus cycles to failure, the data for the three beam types fell onto a single curve at load levels where the remaining prestress after fatigue creep relaxation no longer closed the crack at the minimum load.



## 1. Introduction

Structural elements can fail under either static or fatigue loading. Since concrete structures such as marine structures, parking garages and bridges are subjected to fatigue loading during their lives, it is important to understand their creep and fatigue behaviour. In addition, the limit states (ultimate and serviceability) governed by fatigue behaviour must be taken into account by designers. The primary variable in causing fatigue failure of both steel and composites is the range of applied stress. When a concrete beam is prestressed, the range of stress in the reinforcement is small up to the load at which the concrete cracks. This is because the area of the uncracked concrete in the region of the reinforcement is much greater than that of the reinforcement, and most of the change in force required to balance an applied moment is supplied by a reduction in the compressive stress in the concrete. After cracking, however, the tensile forces required to balance additional moment are supplied by the reinforcement and the stress in the reinforcement increases rapidly and the beam stiffness is reduced.

Glass and carbon fibers have a good resistance to creep; on the other hand, polymeric resins are more susceptible to creep; as a result, fiber type, volume fraction and fiber orientation and temperatures which lead to a decrease in resin strength play an important role in the creep performance of FRP reinforcing rebar.

A study by Noël and Soudki [5] was conducted to investigate fatigue behaviour of GFRP, the results showed that GFRP bars embedded in concrete have shorter fatigue lives than similar bars tested in air by approximately a full order of magnitude.

Preliminary fatigue test results carried out by El Refai [3] showed that the fatigue limit of BFRP bars was about 4% of their ultimate capacity. However, the fatigue limit of GFRP bars was about 3% of their ultimate capacity. Furthermore, the results

* Corresponding author.
*E-mail address:* tyounes@uwaterloo.ca (T. Younes).

https://doi.org/10.1016/j.conbuildmat.2017.09.086
0950-0618/

showed that BFRP has a low sensitivity to water moisture and is a durable material. Therefore, BFRP would be suitable for use as prestressing or non-prestressing.

Compared to steel, the BFRP materials possess a considerable higher strength-to-weight and modulus-to-weight ratios. These properties can be very useful and advantageous for different applications Chemical and mechanical properties of the BFRP material can serve both structural and functional issues pertinent to the particular structure [1]. Therefore, BFRP materials are good candidate for prestress and non-prestress applications. However, a lack of studies on basalt bar reinforced concrete beams in fatigue applications has limited the use of this type of bars in the construction industry. The aim of this study is to investigate the performance of prestressed concrete beams using BFRP bars under monotonic and fatigue loading. Different presetressing levels of bars and fatigue load ranges were investigated.

## 2. Experimental program

Sixteen concrete beams were reinforced with sand coated BFRP bars. The beams that were tested under monotonic and fatigue loading were divided into three groups. The first group had six non-prestressed beams. The second group had six beams that were prestressed to a bar stress of 40% (582 MPa, 71 kN) of the material's static tension capacity as listed in Table 1 and the third group had four beams that were prestressed to a bar stress of 20% (291 MPa, 35.5 kN) of the materials tension capacity. Two beams, one from the first group and the other one from the second group were monotonically loaded to failure under deflection control at a rate of 1 mm per minute and served as a control for all groups, because the expected ultimate load capacity for the third group under monotonic loading is the same as the other two groups. The expected mode of failure for both prestressed and non-prestressed beams was by the bar rupture.

### 2.1. Test specimens

Six beams were non-prestressed and ten beams were pretensioned (six prestressed to 40% and four to 20%). The beam dimensions were 2400 mm in length and 300 mm in height and 150 mm in width, as shown in Fig. 1. All of the beams were simply supported over a length of 2200 mm center to center and subjected to two equal central loads, spaced 300 mm apart, to produce a constant moment region in the middle of the beam. This configuration which creates two equal shear regions with lengths of 950 mm each was designed to avoid bond failure and ensure flexural failure through bar rupture. All of the beams were reinforced with one basalt bar in the tension region with a diameter of 12.45 mm. Two 10 M Grade 400 deformed steel bars were provided in the compression zone. The clear concrete cover of 35 mm was kept constant for all the beams. In order to avoid shear failure and ensure a flexural failure, adequate shear reinforcement was provided in the form of 10 M stirrups spaced at 100 mm center to center.

### 2.2. Instrumentation and prestressing procedure

Sixteen concrete beams were cast and tested. The control beam was loaded monotonically to failure; the load was applied by a hydraulic jack through a load cell, and a steel spreader beam that transferred the load to the test beam. All the beams were loaded in four- point bending as shown in Fig. 2. Nine strain gauges were used in one of the prestressed beams (40% prestressing), which was tested under monotonic loading. The gauges were fixed on the tension reinforcement, three of which were in the constant moment region and three in each of the two shear spans at distances of 100 mm, 250 mm, and 500 mm from the support to measure the strain in the tension reinforcement during prestressing and flexural loading. For the other nine beams a total of 5 strain gauges used. Three strain gauges were placed on the tension reinforcement in the moment constant region only, two of which were placed under the point loads on each side and one was mounted in the middle of the moment constant region. In order to fix the strain gauges, the sand coating of the rebar was removed and the surface of rebar was flattened and cleaned. Then the strain gauges were coated with wax in order to protect them from any damage during casting. The other two strain gauges were mounted on the concrete, one at the top of the concrete at the center of the moment constant region and the other one in the middle of the concrete compression region at the center line of the beam. A linear variable differential transducer (LVDT) was placed at the mid span of the beam to measure the deflection. Ten basalt rebars were prestressed. Six of them were prestressed to 40% of their ultimate capacity and four basalt rebars were prestressed to 20% of their ultimate capacity. Anchorage components used for prestressing are shown in Fig. 3.

To eliminate a stress concentration that can lead to premature failure in the anchor zone, at the interface between the grip and the prestressed bars, the BFRP bars were stressed using a prestressing system having an anchor designed to eliminate this problem developed at the University of Waterloo [2]. The surface at the end of each BFRP bar was cleaned using acetone before anchoring. In order to distribute the stress on the surface of the bar and prevent the wedges from notching the bar, copper sleeves were placed on the bar and then three steel wedges were pushed firmly into the barrel of the grip after they had been assembled around the sleeve. To reduce the friction between the barrel and the wedges, the outer surface of the steel wedges was lubricated with G-n Metal Assembly Paste, and then the wedges were seated into the barrel that was fitted into a steel plate using a hydraulic jack as shown in Fig. 4.

**Table 1**
Mechanical properties of BFRP bars [6].

| Specification | Sand coated Bars |
|---|---|
| Diameter (mm) | 12.45 |
| Ultimate tensile capacity (MPa) | 1456 |
| Modulus of elasticity (GPa) | 53.3 |
| Actual area ($mm^2$) | 121.7 |

### 2.3. Material properties

The mechanical properties of the sand coated BFRP rebars, were determined from a tensile test conducted at the University of Waterloo [6] as reported in Younes et al. [7]. The tested beams were cast from two batches of concrete. All of the 20% and 40% prestressed beams, were cast from one batch; however, the non-prestressed beams were cast from the other batch. The concrete used for the beams was designed to achieve a target compressive strength of (55 MPa) after 28 days. For each of the sixteen beams, cylinders with dimensions of 100 mm in diameter and 200 mm in height were cast and tested to determine the compressive strength of the concrete. Five cylinders were tested at the time of releasing the prestressed bars, and another five were tested 28 days after the pouring of the beams. For the prestressed beams, the average compressive strength after 28-days for five cylinders of the concrete was 50 MPa. For the non-prestressed beams, the average after 28 days was found to be 55 MPa. The mechanical properties of the basalt bars are shown in Table 1.

### 2.4. Loading scheme

In order to study the effect of prestressing level (0%, 20% and 40% of the bar failure load) on the fatigue life of BFRP reinforced beams, five beams of the first group, five beams of the second group, and four beams of the third group were subjected to fatigue loads under load-control.

The minimum load in the load cycle for the fatigue beam specimens was kept equal to 10% of the 85 kN ultimate strength of the control beams and the maximum load was varied for all the tested beams from 11.5% to 80% of the ultimate strength of the control beam (85 kN). The test frequency for all tests was 3.5 Hz. One beam from each of groups two and three was tested again at a higher load range after it had reached the run out limit (1,000,000 cycles).

## 3. Experimental results

### 3.1. Static results

#### 3.1.1. Non-prestressed concrete beam

The first specimen tested under monotonic load was a non-prestressed beam which served as a control beam for the non-prestressed beams. Its load versus deflection curve is shown in Fig. 3. The concrete cracked at a load of 10 kN. The first hairline cracks appeared in the form of flexural cracks in the constant moment region. Four cracks occurred at the same time, two in the middle of the constant moment region and the other two just outside of the constant moment region. At this point, the slope of the load deflection curve decreased indicating that the flexural stiffness of the beam had decreased.

As the load increased, more flexural cracks appeared in the two shear spans of the beam. Then a longitudinal crack occurred on the bottom of the mid-span of the beam at a load of 38 kN. The cracks in the constant moment region grew vertically as the load increased. When the load reached 85 kN, which was slightly lower than the expected ultimate load 90 kN, the basalt rebar ruptured, as expected, followed immediately by crushing of the concrete at the top of the beam.

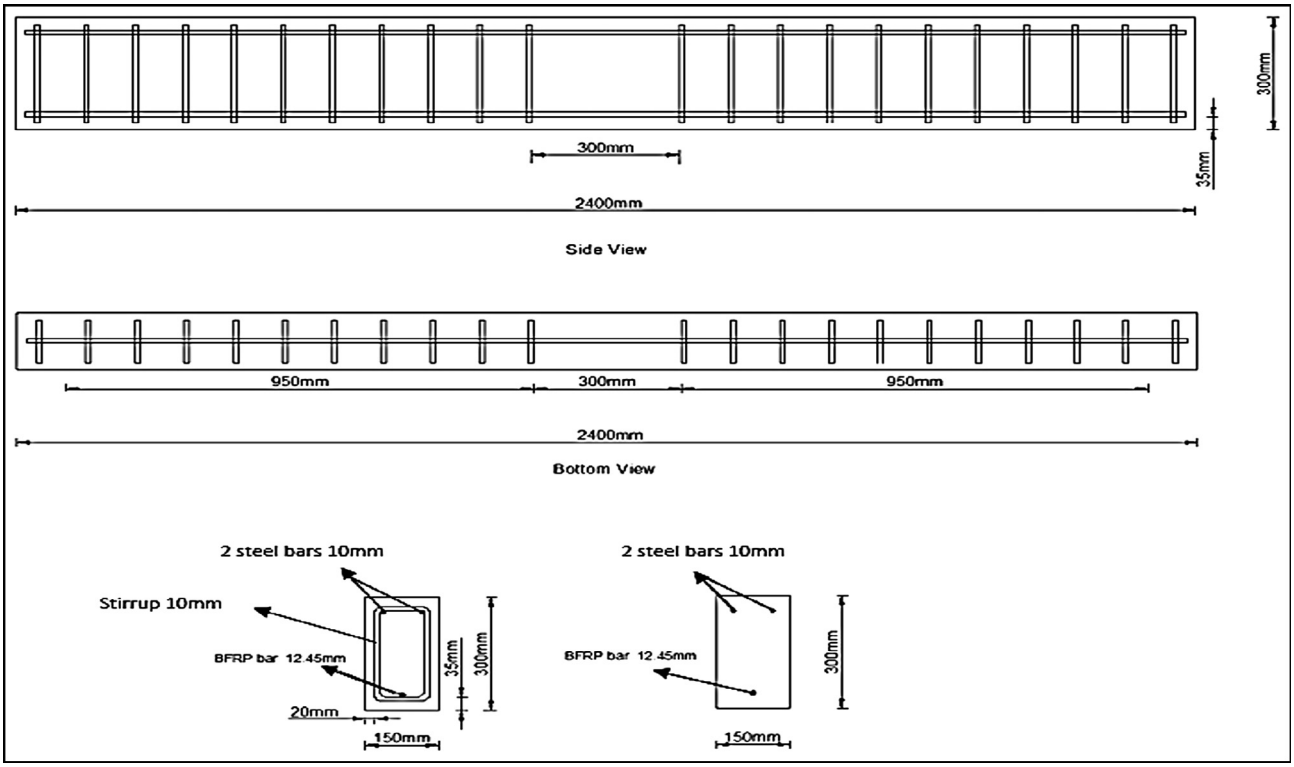


**Fig. 1.** Typical beam configuration.

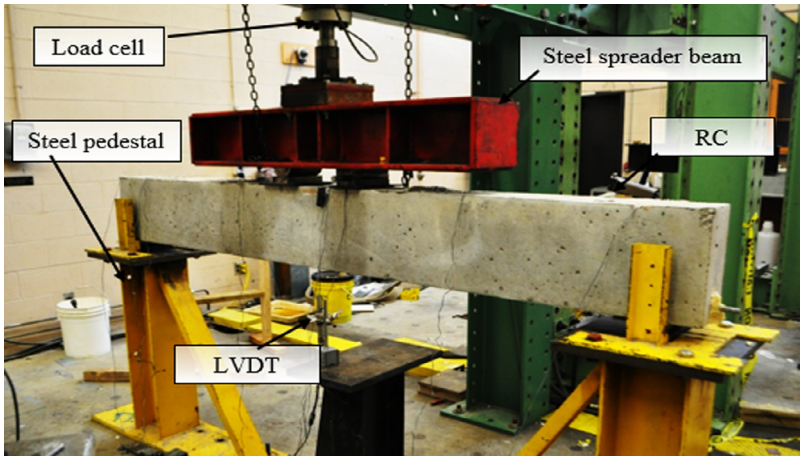


**Fig. 2.** Beam test set up.

*3.1.2. 40%Prestressed beams*

The same set up and loading conditions that were used in the previous beams were followed in testing these specimens**.** One beam prestressed to 40% of tensile bar strength was loaded monotonically to failure and served as a control for the prestressed beams. The load versus deflection curve for the test is shown in Fig. 5. It was expected that this beam would exhibit the same ultimate capacity as the non-prestressed beam; however, the cracking load was expected to be higher. As for the previous beam, the first hairline flexural cracks appeared in the tension region of the beam. They started to form when the tensile stress in the concrete had exceeded its tensile strength at an applied load of 33 kN, which was lower than the expected cracking load of 45 kN that was calculated using Eq. (1). Cracks were observed in the moment constant region and just outside of the constant moment region and the slope of the load-deflection curve decreased; as a result of the decreased flexural stiffness of the beam.

Then flexural cracks occurred on both sides of the shear spans of the beam when the load reached 40 kN followed by a sudden formation of longitudinal cracks at the midspan on the bottom face of the beam. At 45 kN all of the strain gauges failed.

The cracks outside of and in the constant moment region grew vertically as the load increased. When the load reached 85 kN, a compression failure occurred with crushing of the concrete at the top of the beam, then the load dropped until bar rupture and complete collapse of the beam took place at a load of 65 kN. The expected bar rupture as a mode of failure did not occur. Reasons for the change to concrete crushing from the expected bar failure may be the close proximity of the provided reinforcement ratio to the balanced ratio, (0.00316 and 0.00359, respectively). Also,


**Fig. 3.** Anchorage components used for prestressing.

**Fig. 4.** Hydraulic manual pump and jack used in pre-seating the anchor.

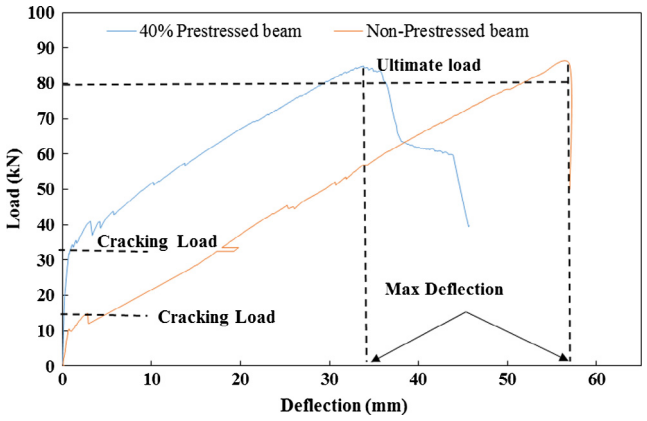


**Fig. 5.** Load-deflection curve for non-prestressed and pre-stressed beam.

the concrete compressive strength of 50 MPa after 28 days was less than the design value of 55 MPa.

$$M_{cr} = \left(0.6 * \sqrt{f_c} + (P/A_g) + (P * e * Y_b)/I_g\right) * (I_g/Y_b) \quad (1)$$

where

$I_{cr}$ = moment of inertia of cracked section, $A_g$ = gross area of the beam cross-section,
$I_g$ = gross section moment of inertia, $e$ = eccentricity of an internal prestressing tendon,
$P$ = effective value of the prestress force, and $Y_b$ = distance from the extreme bottom fiber to the centroid of the gross section.

### 3.2. Prediction of the fatigue life

The predicted fatigue life for the non-prestressed and pre-stressed beams was calculated as follows:

1. A cracked section strain compatibility approach analysis was used to calculate the stress ranges in the reinforcing bar for each of the beam tests (bars imbedded in concrete). Then, the losses of prestress due to cyclic creep strain of the imbedded basalt bars in concrete were calculated from the half-life fatigue creep strain curve for the bare bars shown in Fig. 6. Fig. 6 was obtained by testing the bars in air under fatigue test to determine the creep strain of theses bars as shown in Fig. 7. Eq. (2) describes the relationship between the cyclic creep strain at one-half of the fatigue life, and the stress range for tests with stress ranges of 50%, 45% 35%, 26.4%, 19% and 15% of the ultimate capacity of the basalt rebar. The bars have length of 630 mm and diameter of 12.45 mm. The fatigue creep strain, taken at one-half of the fatigue life is given by:

$$\sigma = \begin{cases} 35.029\varepsilon, & for \quad 0 \leqslant \varepsilon < 0.0097 \\ 1.8119\varepsilon + 0.2164, & for \quad 0.0097 \leqslant \varepsilon \leqslant 0.145 \end{cases} \quad (2)$$

2. The stress ranges that were obtained from step 1 after taking into account the changes in stress range due to cyclic creep were entered in the stress range versus fatigue life curve of Fig. 8 to obtain fatigue life predictions f or the proposed beam tests using Eq. (3).

$$\sigma = \begin{cases} K_1 * N^{-B_1} & for \quad 1 \leqslant N < 2000 \\ K_2 * N^{-B_2}, & for \quad 2000 \leqslant N \leqslant 1000000 \end{cases} \quad (3)$$

where: $K_1 = 0.9109$ and $K_2 = 3.9249$ are the intercept, $B_1 = 0.102$ and $B_2 = 0.292$ are the slope, N is the number of cycle.

Fig. 8 was obtained by testing 3 bare basalt bars to failure under monotonic loading. The bars have length of 630 mm and diameter of 12.45 mm. The average ultimate load of the machined bare bars under monotonic loading is 176.3 kN and the average modulus of elasticity is 53.3 GPa as shown in Table 2. Also, Nine BFRP bars were tested under fatigue loading. The stress ranges varied from 7.5% to 57% of the ultimate capacity of the basalt bars. The minimum stress for all tests was kept constant at 40% of the ultimate capacity of the bare bars. The bar that was tested at a stress range of 7.5% of the ultimate capacity of the bar failure load ran out to one million cycles.

Table 3 summarizes the fatigue lives for the bare basalt bar tests. In Fig. 8, the blue dots on the show a high stress region where the extensive fatigue creep led to failures at lives that fell below an extension of the linear log -log curve for long life fatigue failures.

#### 3.2.1. Non-prestressed beams

Five non-prestressed beams were tested under fatigue loading. The load range varied from 11.5% (9.78 kN) to 45% (38.25 kN) of the ultimate static capacity of the beam (85 kN). The maximum load varied between 21.5% and 55% of the ultimate static capacity of the beam (between 18.27 kN and 46.75 kN). However, the minimum load was kept constant for all the beams and set to be 10% (8.5 kN) of the ultimate static capacity of the control beams. At the outset of each test, all of the beams were first loaded to the maximum load and then back to the mean load manually. While loading to the maximum load, flexural cracks were observed in and outside the constant moment region for all beams. During

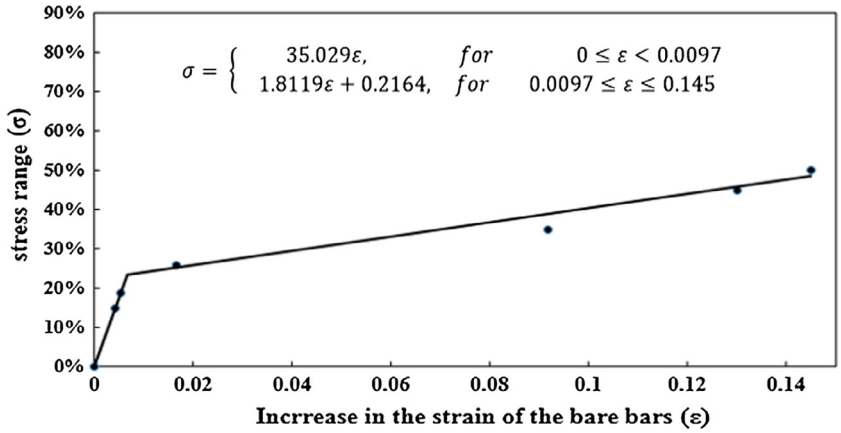


**Fig. 6.** Fatigue creep strain of bare basalt bars at different stress ranges.

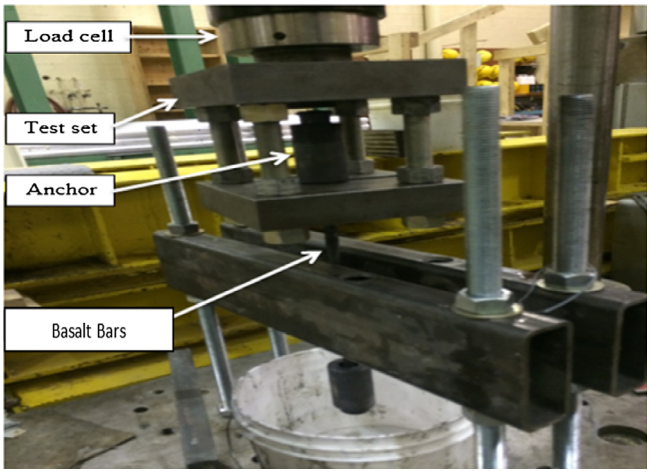


**Fig. 7.** Bar in test frame with wedge anchorage.

cycling, flexural cracks propagated and grew vertically and a longitudinal crack initiated on bottom face at the midspan of the beam.

The beam tested at 11.5% (9.78 kN) of the failure load of the control beam failed by bar rupture at 650,000 cycles. The extrapolated run out load range at one million cycles was 9% of the failure load of the control beam. The rest of the beams in this series were tested at load ranges equal to 14%, 18%, 25%, and 45% of the control beam failure load. All of these beams failed by bar rupture in this series - none of the beams ran out.

Inspection of the broken bars and adjacent concrete pieces showed that the sand coating was sheared off from the bars and in some places still adhered to the concrete pieces. The bars showed surface scratches indicative of fretting between the sand or the surrounding concrete and the bar as shown in Fig. 9. A similar failure mechanism has been reported by Katz [4] and Noël and Soudki [5] who described extensive shearing off the sand coating and fretting of their GFRP bars.

### 3.2.2. 40% prestressed beams

Five beams with their bars prestressed to 40% of their tensile strength were tested under fatigue loading. Before starting load cycling, all beams were first loaded to the maximum load in the load cycle and back to the mean load manually. During loading, flexural cracks appeared in and close to the constant moment region for all beams except for the beam that was tested at a load range of 20% (17 kN) of the control beam failure load and ran out to one million cycles which had no cracks. While the beams were cycled, flexural cracks propagated and grew vertically and a longitudinal crack initiated on the bottom faces at the midspan of the beam. The beam tested at the lowest load range (20% of the control beam failure load) ran out to the one million cycle limit chosen and

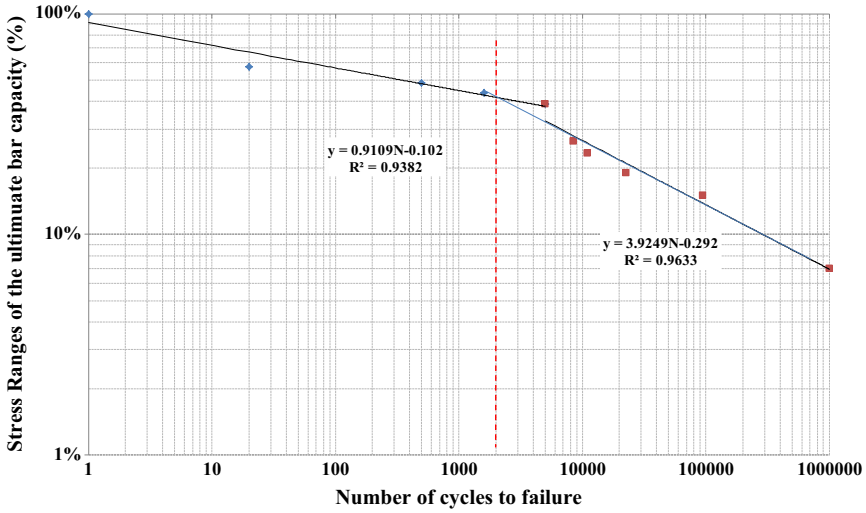


**Fig. 8.** Fatigue life of bare basalt bars.

**Table 2**
Monotonic test results of bare BFRP bars.

| Test number | Ultimate load (kN) | Ultimate stress (MPa) | Elastic modulus (GPa) |
|---|---|---|---|
| 1 | 173 | 1421.5 | 52.5 |
| 2 | 177 | 1456 | 53.3 |
| 3 | 180 | 1479.0 | 54.1 |
| Average | 177 | 1452 | 53.3 |

was retested at the highest fatigue load range of 80% of the control beam failure load where it failed after 184 cycles. In this test, the failure mode was by concrete crushing followed by bar rupture 14 cycles later. The expected bar rupture mode of failure did not occur possibly because the first million cycles had no effect on the BFRP strength since the beam did not crack, and then when the high load range was applied in the second series of loading, the load was high and close enough to the static failure load to quickly cause failure by the same mode due to the compression force induced by prestresssing. The other four beams were tested at load ranges of 27%, 35%, 47.5% and 60% of the control beam failure load. All of these beams failed by bar rupture.

Similar to the previous specimens (non-prestressed beams) in this test series, an investigation of the broken bars showed that the sand coating was sheared off the bars and in some places was stuck firmly to the concrete pieces as shown in Fig. 10.

### 3.2.3. 20% prestressed beams

Four beams with their bars prestressed to 20% of their tensile strength were tested under fatigue loading. As with the previous beams, they were loaded to the maximum load and then unloaded to the mean load before fatigue loading began. The fatigue load ranges used were 13%, 18%, 26%, 55% and 70% of the control beam failure load. During loading, flexural cracks appeared in and close to the constant moment region for all beams except for the beam that was tested at a load range of 13% (11 kN) of the control beam failure load and ran out to one million cycles which had no cracks and it was retested at a load range of 70%. Again, the minimum fatigue load was fixed for all the beams at 10% (8.5 kN) of the maximum capacity of the control beam. The retested beam at a load range of 70% of the control beam failure load failed by concrete crushing. All of the other beams failed by bar rupture. As observed for the previous beams, flexural cracks propagated and grew vertically. In addition, a longitudinal crack initiated on the bottom faces at the midspan of the beams during testing except for the beam tested at a load range 13% which did not exhibit any cracking. Also, as for the previous beam series, the bars of the failed beams showed scratching indicative of fretting.

## 4. Discussion

Table 4 gives a summary of the fatigue lives of all the tested beams (non-prestressed, 20% prestressed and 40% prestressed) together with the expected fatigue lives calculated from bare basalt bar fatigue data in the previous section. The fatigue test results for the three sets of beams are plotted on logarithmic axes of load range versus cycles to failure as shown in Fig. 8 together with the predicted fatigue lives. In Fig. 8, fatigue results show two different slopes. The flat portion of the curves in the low stress long life region indicates that the crack is closed and the applied load is below the decompression load, where the tensile stress at the bottom fiber of concrete beam is equal to zero. Below this level, the compression force in the beam is shared by the bar and the concrete greatly increasing the beam stiffness and decreasing the change in bar stress with changes in load. However, at higher load levels the crack is open so that all the tensile force is carried by the bar and the applied stress ranges are proportional to the load ranges.

The non-prestressed beam tested under monotonic load failed by bar rupture. Also, the beam prestressed to 40% of the ultimate capacity of the rebar tested under monotonic load failed by the concrete crushing (CC). Moreover, the 20% and 40% prestressed beams at the highest fatigue load levels failed by concrete crushing. For the rest of the beams, failure was by fatigue failure of the bars in a form of bar rupture (BR).

Fatigue data for beams at the two levels of prestressing and for the non-prestressed beams fall into a compact band in the life region between 1000 and 100,000 cycles as shown in Fig. 11. This band is parallel to, but at fatigue lives more than twice, those predicted from the bare bar fatigue data [7]. The discrepancy can be attributed to the stress concentration imposed by the end gripping

**Fig. 9.** Sand coating sheared off the basalt bars.

**Table 3**
Summary of fatigue lives for the bare basalt bar.

| Notation* | Min load (kN) | Max load (kN) | Load range (kN) | Fatigue life (cycles) | Stress range (%) |
|---|---|---|---|---|---|
| | – | 177 | 177 | 1 | 100 |
| FBB-1 | 71 | 171.69 | 100.69 | 20 | 57 |
| FBB-2 | 71 | 157.33 | 86.33 | 500 | 48.7 |
| FBB-3 | 71 | 148.72 | 77.72 | 1600 | 43.89 |
| FBB-4 | 71 | 140 | 69 | 5047 | 39 |
| FBB-5 | 71 | 118 | 47 | 8444 | 26.4 |
| FBB-6 | 71 | 112.5 | 41.5 | 10,977 | 23.4 |
| FBB-7 | 71 | 105.21 | 34.21 | 22,683 | 19 |
| FBB-8 | 71 | 97.84 | 26.84 | 94,323 | 15 |
| FBB-9 | 71 | 84.56 | 13.56 | 1,000,000 | 7.5 |

* FBB: Stands for fatigue bare basalt bar, and the last number refers to the number of the specimen.

**Fig. 10.** Adherence of sand coating of basalt bars to the concrete surface.

**Table 4**
Fatigue test results for all the tested beams.

| Description | Notation* | Load range (%)** | Min. stress (MPa) | Max. stress (MPa) | Stress Range (%) | Expected fatigue Life | Expected failure mode | Actual fatigue life (cycle) | Failure mode*** |
|---|---|---|---|---|---|---|---|---|---|
| Non-Prestressed Beams | F-0%-45 | 45 | 133 | 734 | 41 | 1000 | BR | 3343 | BR |
| | F-0%-25 | 25 | 133 | 467 | 23 | 10,000 | BR | 19,500 | BR |
| | F-0%-18 | 18 | 133 | 347 | 17 | 35,000 | BR | 64,176 | BR |
| | F-0%-14 | 14 | 133 | 321 | 13 | 100,000 | BR | 242,802 | BR |
| | F-0%-11.5 | 11.5 | 133 | 288 | 11 | 250,000 | BR | 650,000 | BR |
| 40% Prestressed Beams | F-40%-80 | 80 | 133 | 1240 | 76 | 100 | BR | 184 | CC |
| | F-40%-60 | 60 | 133 | 970 | 57 | 300 | BR | 1218 | BR |
| | F-40%-47.5 | 48 | 133 | 800 | 46 | 800 | BR | 4044 | BR |
| | F-40%-35 | 35 | 133 | 635 | 34 | 2500 | BR | 8363 | BR |
| | F-40%-27 | 27 | 293 | 590 | 20 | 20,000 | BR | 29,545 | BR |
| | F-40%-20 | 20 | 435 | 573 | 9 | 300,000 | BR | 1,000,000 | Run Out |
| 20% Prestressed Beams | F-20%-70 | 70 | 133 | 1377 | 65 | 190 | BR | 146 | CC |
| | F-20%-55 | 55 | 133 | 1080 | 51 | 500 | BR | 1330 | BR |
| | F-20%-26 | 26 | 133 | 880 | 23 | 10,000 | BR | 20,574 | BR |
| | F-20%-18 | 18 | 133 | 475 | 18 | 22,000 | BR | 99,250 | BR |
| | F-20%-13 | 13 | 171 | 390 | 9 | 300,000 | BR | 1,000,000 | Run Out |

Notations:
* F stands for fatigue, 0% non-prestress, 40% prestressing level, and 20% prestressing level, and the last number refers to load range.
** Percentage of ultimate static load.
*** BR: Basalt Bar Rupture.

of the bare bars. The fatigue test results indicated that there was almost no benefit from prestressing in this life region. In the fatigue life region above 100,000 cycles, the predicted and observed fatigue strengths increased with the prestress level. The fatigue endurance limits, below which failure does not occur, fell close to the cracking loads of the beams. For the tests at shorter lives where prestressed and non-prestressed beams fell on a single band, calculations of the prestress after fatigue creep indicated that the prestress decreased enough during cycling that the crack did not close at the minimum load and all beams were exposed to the same stress range at a given load range.

Beam fatigue data for the non- prestressed and two prestress levels is compared to the fatigue data for the bar specimens (not encased in concrete), as shown in Fig. 12. For the bar tests the minimum load was kept constant for all the specimens at 40% of the ultimate bar capacity. The minimum stress in the bar was calculated using Eq. (4) for the fatigue tests of prestressed beams since at this load level the cracks were closed as a result of the prestress. The reason behind using 40% of the monotonic failure stress as the minimum stress in the bar fatigue tests was to derive data applicable to the bars in beams prestressed to 40% of the ultimate bar capacity (a level typically used in beams in service).

$$f = (M * Y_e/I_g) * n + f_{pe} \quad (4)$$

where: $f$ = Minimum stress in BFRP bar.
$M$ = Applied moment.
$Y_e$ = Distance from the elastic centroid of a transformed section to the location of a BFRP bar.
$I_g$ = Gross transformed section moment of inertia $f_{pe}$ = Effective prestress after losses, including elastic shortening. The initial prestress level was 40% of the ultimate capacity of the rebar.
$n$ = Modulus ratio = $(E_{frp}/E_c)$.

The bar fatigue data as expected show lower fatigue strengths at all fatigue lives than the beams. The curve drawn through the bar fatigue data falls parallel to the beam fatigue data at about one half the fatigue lives of the beams. In Fig. 12, the fatigue data is plotted in terms of stress range versus life and falls on a single curve. Cracked section analysis was used to calculate the stress

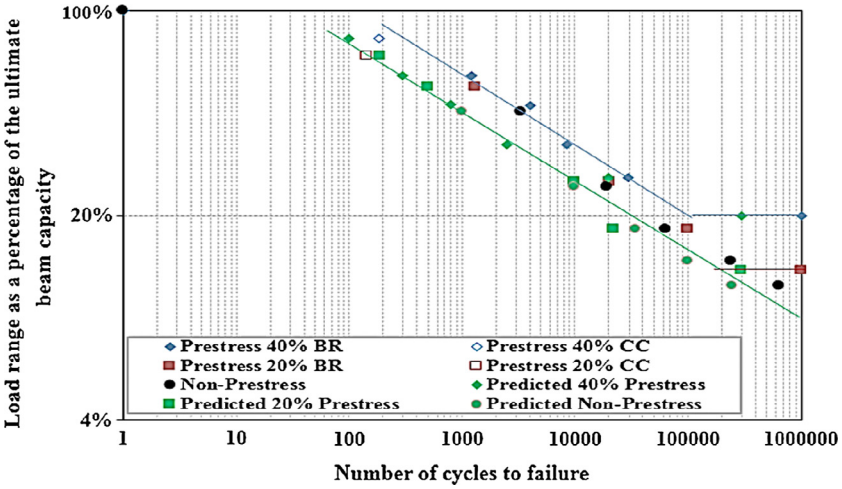


**Fig. 11.** Measured and predicted fatigue life of non-prestressed, 40% and 20% prestressed beams.

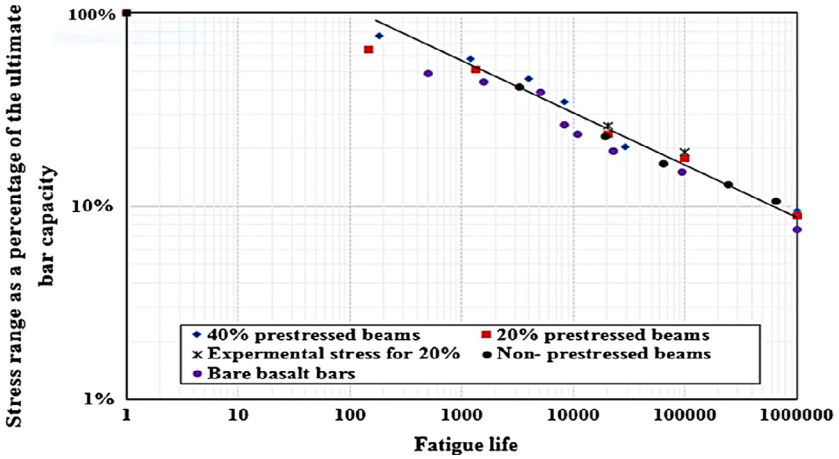


**Fig. 12.** Fatigue lives for bare basalt bars (at a minimum stress level of 40% of the ultimate bar capacity), and for non- prestressed beams and for beams with two levels of prestress (20% and 40% of the ultimate bar capacity).

ranges, which are proportional to the load ranges except when cracks close. Below this level Eq. (4) was used to calculate the stresses.

## 5. Conclusions

A total of 16 beams reinforced with non-prestressed and prestressed basalt bars were tested to failure. The first series consisted of six non-prestressed beams. The second series had six beams prestressed to 40% of the ultimate strength of the BFRP bar and the third series had four beams prestressed to 20% of the ultimate strength of the BFRP bar. All of the beams were tested under fatigue loading in load control except two beams, one from the first series and the other from the second series that were tested under monotonic loading in displacement control.

A number of conclusions and recommendations were drawn from the experimental results:

1. For fatigue lives less than 100,000 cycles, there was no improvement in fatigue strength due to prestressing. At the stress ranges in the bars in this life range, results of fatigue tests indicated that due to the loss of prestress caused by creep, crack closure due to the remaining prestress would fall below the minimum load in the test cycle. However, at fatigue lives above 100,000 cycles creep, calculations indicated that enough prestress was retained to close the crack above the minimum load and prestress significantly increased the fatigue strength of both 20% and 40% prestressed beams.
2. The mode of failure of the prestressed beam reinforced with BFRP rebar tested under monotonic loading was due to the concrete crushing followed by bar rupture. This unexpected result may be because the concrete compressive strength of 50 MPa was lower than the target compressive strength of 55 MPa.
3. The mode of failure of the non- prestressed beam under monotonic loading was by bar rupture followed immediately by concrete crushing at the top of the beam.
4. The mode of failure of the prestressed RC beams reinforced with BFRP rebar tested under fatigue load at the highest load range for both levels of prestressing was by concrete crushing at the top; however, at all lower load ranges failure was by bar rupture.
5. The mode of failure of all the non-prestressed beams reinforced with BFRP bars tested under fatigue load was by bar rupture as expected.
6. Load ranges of 20% and 13% of the monotonic loading strength of the basalt beams respectively are recommended as endurance limits for concrete beams reinforced with 40% and 20% prestressed BFRP, respectively.

## References

[1] S. Adhikari, Mechanical Properties and Flexural Applications of Basalt Fiber Reinforced Polymer (BFRP) Bars (Doctoral dissertation), University of Akron, 2009.
[2] A. Al-Mayah, K. Soudki, A. Plumtree, Development and assessment of a new CFRP rod–anchor system for prestressed concrete, Appl. Compos. Mater. 13 (5) (2006) 321–334.
[3] A. El Refai, Durability and fatigue of basalt fiber-reinforced polymer bars gripped with steel wedge anchors, J. Compos. Constr. 17 (6) (2013).
[4] A. Katz, Bond to concrete of FRP rebars after cyclic loading, J. Compos. Constr. 4 (2000) 137–144.
[5] M. Noël, K. Soudki, Fatigue behavior of GFRP reinforcing bars in air and in concrete, J. Compos. Constr. 18 (2014).
[6] T. Younes, Fatigue Flexural Behaviour of Reinforced Concrete Beams with Non-Prestressed and Prestressed Basalt Fiber Reinforced Polymer Bars (M.A.Sc. thesis), University of Waterloo, Waterloo, Canada, 2015.
[7] T. Younes, A. Al-Mayah, T. Topper, Fatigue performance of basalt fiber reinforced polymer (BFRP) for prestressed concrete, J. Compos. Constr. (2017). submitted paper.